Automation in Construction 139 (2022) 104272

Contents lists available at ScienceDirect

Automation in Construction

journal homepage: www.elsevier.com/locate/autcon

Augmented-reality-assisted timber drilling with smart retrofitted tools

Andrea Settimi *, Julien Gamerro, Yves Weinand

Ecole Polytechnique Fédérale de Lausanne (EPFL), School of Architecture, Civil and Environmental Engineering (ENAC), Institute of Civil Engineering (IIC), Laboratory for Timber Constructions (IBOIS), GC H2 711, Station 18, Lausanne 1015, Vaud, Switzerland

ARTICLE INFO

Keywords:
Timber construction
Digital fabrication
Augmented reality
Assisted fabrication
Tool tracking
Smart tool

ABSTRACT

An ordinary electric drill was integrated into a context-aware augmented reality (AR) framework to assist in timber-drilling tasks. This study is a preliminary evaluation to detail technical challenges, potential bottlenecks, and accuracy of the proposed object- and tool-aware AR-assisted fabrication systems. In the designed workflow, computer vision tools and sensors are used to implement an inside-out tracking technique for retrofitted drills based on a reverse engineering approach. The approach allows workers to perform complex drilling angle operations according to computer-processed feedback instead of drawing, marking, or jigs. First, the developed methodology was presented, and its various devices and functioning phases were detailed. Second, this first proof of concept was evaluated by experimentally scanning produced drillings and comparing the discrepancies with their respective three-dimensional execution models. This study outlined improvements in the proposed tool-aware fabrication process and clarified the potential role of augmented carpentry in the digital fabrication landscape.

1. Introduction

1.1. Context

Full robotic automation and digital fabrication in construction have attracted considerable research attention. Although effective, these technologies require high capital investment, highly qualified operators, and are typically adapted for specific tasks, which restricts their use in unstructured environments and constantly changing workflows. These techniques promise the future digitization of the architecture engineering and construction industry, and they are currently not the most rapid and accessible solutions for small and local construction companies that use bio-sourced materials such as timber. Augmented reality (AR) has attracted considerable interest in fabrication and construction [1]. AR is increasingly being used in hybrid technological formats. This technology combines human dexterity and cognition with digital computation in manual construction processes. Using these digital manufacturing methods, management of existing human resources is digitized for a limited investment in exchange for a high-efficiency payoff [2] and rapid implementation. AR technology is now maturing. Improved industrial head-mounted displays (HMDs), such as Hololens2, with enhanced holographic precision, extensive field of view (FOV), and robust computational features are now commercially available. Advancements in mixed reality headsets can represent reliable alternatives to standard headsets (Lynx-R1 or Varjo-XR 3). Time-of-flight sensors are being integrated into mainstream smartphones, rendering AR stable and accessible to both consumers and developers. Holographic models have been used as augmented 3D templates [3]. Novel efficient feedback loop logic integrated into fully operational augmented frameworks is emerging, particularly in volume additive operations such as bricklaying or building component assembly. Systems such as "augmented bricklaying" [4] exhibit considerable potential for seamless tracking of the position of the physical element and inform the augmented framework of the updated as-built context. This phenomenon is a substantial advancement over previous unidirectional and context-unaware applications in augmented fabrication.

However, compared with augmented volume additive tasks, supplementary conceptual and technological challenges exist for the application of AR in volume subtractive manufacturing. In addition to context awareness features, the physical properties of the tool should be

Abbreviations: AEC, Architecture Engineering and Construction; AR, Augmented Reality; HMD, Head-Mounted Display; FOV, Field of View; ICP, Iterative Closest Point; IMU, Inertial Measurement Unit; IR, Infrared signals; MRTK, Microsoft Mixed Reality Toolkit; SLAM, Simultaneous Localization and Mapping; ToF, Time of Flight; UWP, Universal Windows Platform; UI, User Interface; VIO, Visual Inertial Odometry; 6DoFs, Six Degrees of Freedom.

* Corresponding author.
E-mail address: andrea.settimi@epfl.ch (A. Settimi).

https://doi.org/10.1016/j.autcon.2022.104272
Received 3 August 2021; Received in revised form 24 February 2022; Accepted 16 April 2022
Available online 29 April 2022

recorded in AR volume subtractive systems to enable a reliable feedback loop mechanism during fabrication. Therefore, tool tracking is a crucial factor for the use of state-of-the-art volume subtractive AR for basic timber manufacturing operations, such as drilling, sawing, and sanding.

1.2. Related works

Millimetric tool tracking precision has been achieved through an outside-in monitoring system using infrared (IR) markers [5,6], 3D printed custom markers, and multiple motion cameras [7]. However, outside-in tracking methods require preliminary installation of capture devices in the workspace, which considering the unpredictable environments of construction sites represents a big challenge in the ease of deployment. In other AR applications, the capacity of HMDs is used to track tools previously integrated with fiducial markers [8]. Based on the same logic, attaching a cube or polyhedron to the device where a fiducial tag occupies each face can reinforce tracking robustness [9,10]. Although easy to deploy, this method hinders the operator's field of vision during fabrication. The user should actively ensure that the fiducial marker is in the detection FOV of the AR device. Furthermore, poor lighting conditions can result in incorrect detection, particularly for small targets. In a previous study, handheld drills equipped with magnetic motion tracking systems were developed for direct streaming into a stationary computer, which directed the correct execution of the 3D model through drill-bit speed control [11]. Such embedded and haptic systems are easy to deploy and are becoming increasingly popular because of the democratization and low cost of microprocessors and components, such as gyroscopes, accelerometers, or magnetic motion sensors [12,13]. Although some customer-oriented smart tools already exist [14], handheld robotic devices are still in a nascent stage. However, they exhibit considerable potential for data-driven manufacturing, especially if coupled with context-aware systems.

Although not yet directly applicable to tool tracking, research on the indoor localization of small-sized autonomous robotic systems, such as drones, has some relevance to our application. For indoor applications, autonomous system localization should rely on data other than GPS signals. As an alternative, commercial standalone simultaneous localization and mapping (SLAM) systems can provide position and orientation information in internal environments by coupling multiple sensor feeds produced by a gyroscope, accelerometer, and visual inertial odometry (VIO). SLAM systems can be used for object avoidance [15] and 3D scanning applications when coupled with RGB-D cameras [16]. Moreover, a study using event-based cameras, a particular bio-inspired sensor that provides an asynchronous stream of frames, revealed a method to obtain a stable six-degrees-of-freedom (6DoFs) stream from these sensors even under extreme motion conditions [17]. As in drone localization, in-hand tool tracking exhibits similar challenges for vibrations, abrupt motion events, small tolerances, autonomous inside-out and markerless tracking, and limited room and weight for sensor installation. As a preliminary pilot study, this study tests the pertinence and efficacy of well-established visual inertial tracking methods in handheld drill tracking.

1.3. Objectives

This study details how execution shop drawings, hand markings, and physical jigs in woodworking can be replaced by an augmented framework featuring tool and object tracking systems. With such implementations, workers can perform complex drilling angle operations by following computer-processed feedback instead of physical guides or holographic templates [18]. First, the developed methodology is presented in the following section along with its devices and functioning phases. Second, this first proof of concept was evaluated with an experimental campaign consisting of 3D scanning of the produced drillings and comparing the intensity of discrepancies with their respective 3D execution models. Finally, the last section outlines potential improvements and new perspectives for augmented carpentry.

2. Developed methodology

The presented setup for augmented drilling consists of three primary devices, each responsible for a specific task of the process (see Fig. 1): (1) an electric drill retrofitted with a self-tracking camera (Intel® RealSense™ Tracking Camera T265 [19]); (2) an AR HMD (Microsoft HoloLens 2) providing a hands-free user interface (UI) and a visualization of the 3D execution model through a deployed Universal Windows Platform (UWP) application on the device; and, (3) a laptop collecting and processing data streams from both the tool sensors and the headset to assist the operator in correcting the drill position, orientation, and depth of the hole. In this context, the augmented drilling operation occurred in three temporally distinct phases. First, the timber stock was 3D scanned, and the corresponding 3D shop drawings were produced. Second, the drill was embedded with sensors and integrated into the augmented framework. Third, augmented drilling operations were performed.

2.1. Timber stock acquisition and execution drawings

The timber stock was digitized in batches using a handheld IR-based scanner (FARO® Freestyle2) to obtain digital replicas of physical objects. Although time-consuming, the employed high-definition scanning (0.5 mm under 1-m distance of capture) allows us to model every irregularity constantly even in off-shelf sawn-timber elements. In the future, lighter pipelines should be developed to seamlessly integrate contemporary carpentry logistics.

The captured raw point clouds were imported into the Rhinoceros 3D modeling workspace and processed using Cockroach [20], an open-source NET-based toolkit for point cloud manipulation, and advanced postprocessing in CAD environments (see Fig. 2 (A)). The raw data were segmented using the library to obtain individual point clouds for each

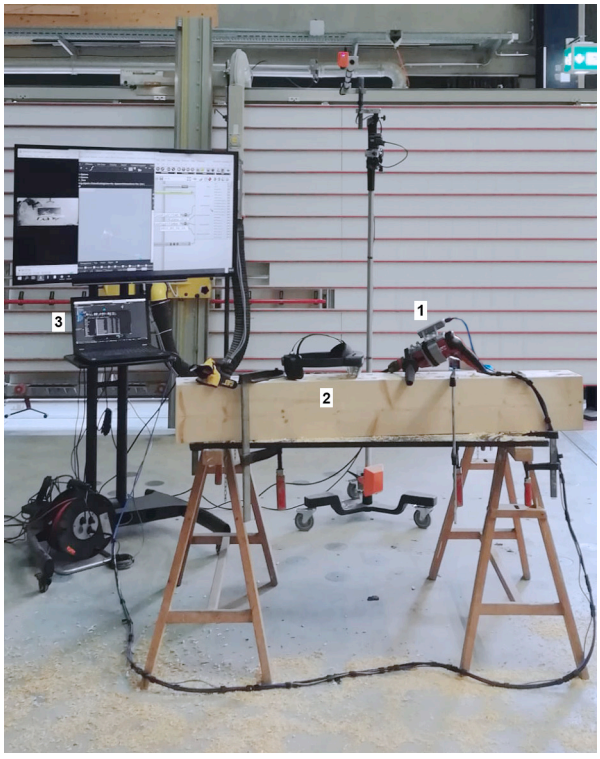

Fig. 1. Experimental augmented drilling workspace: (1) enhanced drill with the inertial measuring unit (IMU) camera installed on a three-dimensional (3D) printed mount, (2) augmented reality headset for hands-free holographic interface visualization, and (3) laptop for data live-stream processing.

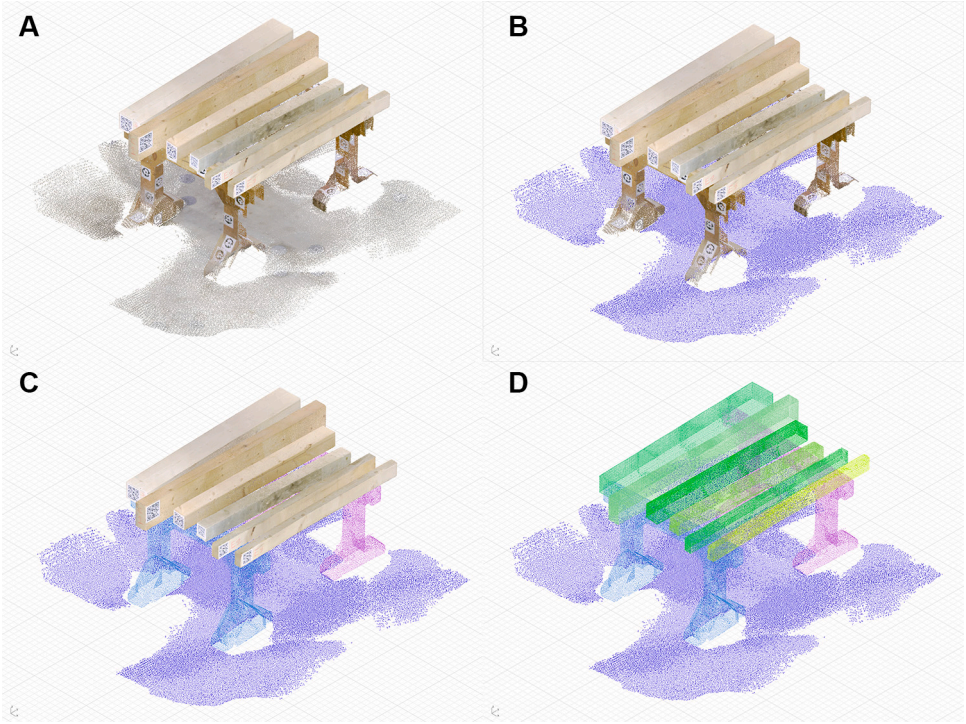

Fig. 2. (A) Raw point cloud imported as a .E57 file into the Rhinoceros workspace, (B) ground is segmented from the point cloud, (C) pre-scanned stands are fit into the scene to segment the corresponding areas of the point cloud, and (D) timber elements are segmented through Euclidean clustering.

timber element (see Fig. 2).

The success of AR fabrication systems typically depends on the capacity of the augmented framework to overlay physical objects and numerical data. Studies have proposed the use of markers at fixed and known locations of the component [21] or using multiple markers as reference points to align predictable, regular geometries to overcome this problem [22]. Although future applications will most likely focus on markerless approaches, this study investigated high-resolution scanned

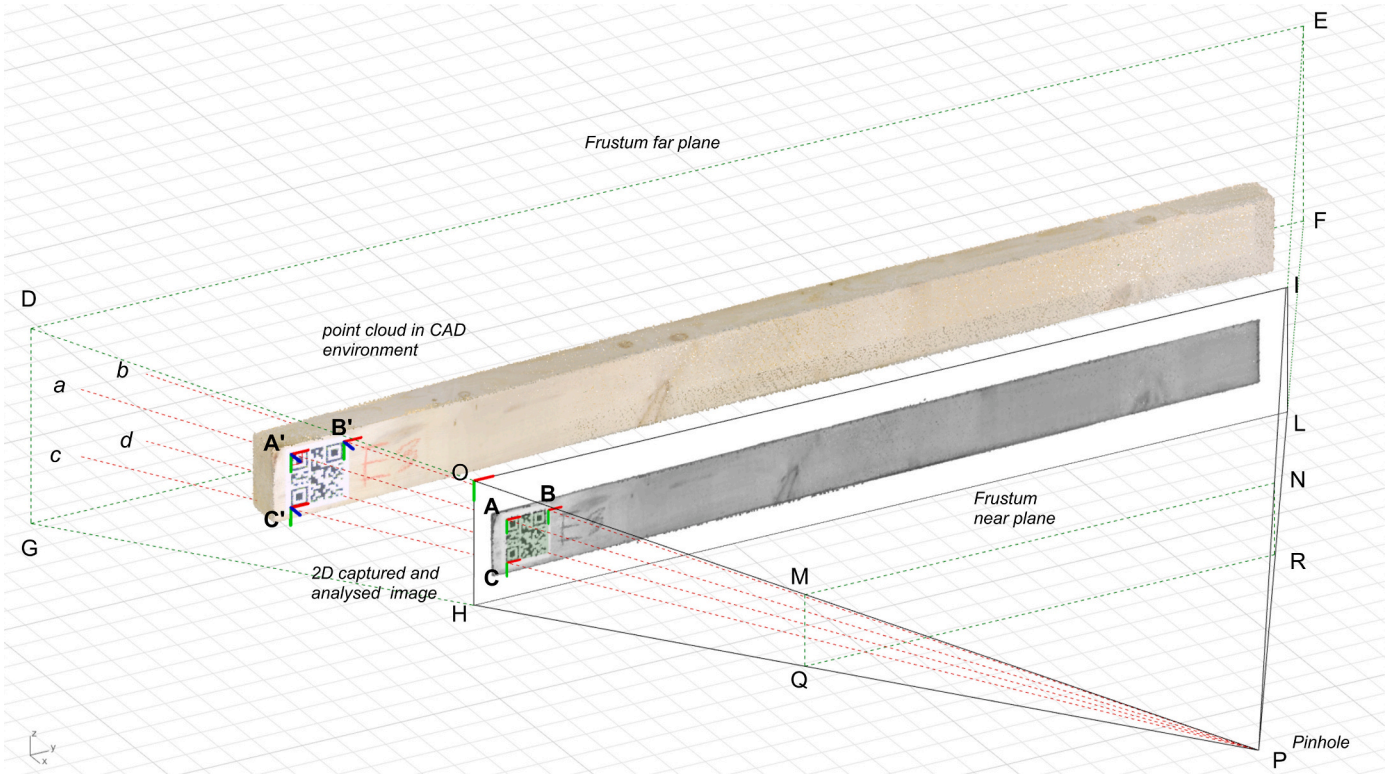

Fig. 3. Computer vision analysis on point clouds within a CAD virtual 3D space (e.g. marker detection). In the proposed method, the absence of camera intrinsics is used to seamlessly run image analysis on point clouds and embed them with 3D dimensional additional information such as the presence and 6DoFs pose of a marker.

point clouds to improve the precision of the marker-based alignment method.

Before scanning, timber elements were labeled with a QR code marker at an unspecified position and orientation on their surface. When the point cloud is acquired, because of its high definition, the marker can be easily detected using the OpenCV library (see Fig. 3). Because of the known virtual pinhole position in the CAD frustum and the absence of intrinsic camera parameters (see Fig. 3, P), the 2D pixel results were converted into 3D Cartesian coordinates. Thus, real-world marker orientation and position were recorded (see Fig. 4). QR code detection was implemented on one of the four gray-scale micro cameras present on the HMD. By avoiding the use of the primary frontal camera, the device rendering frame rate was constantly kept stable at 60 fps even during detection tasks, resulting in the display of stable holograms during fabrication.

When all postprocessing operations are completed (see Fig. 5A) and the execution drawings are ready (see Fig. 5B), the CAD filar geometries are converted using a Grasshopper C# scripted component into a structured list of points coordinates stored in an XML file (see Fig. 5 (C)). Because of the limited computational power of the HMD, the timber CAD volumes are not represented by meshes, but instead by their top-end outlines. After conversion, the mark-up text files are transferred to a storage cloud service that is ready to be accessed by the operator subsequently in the fabrication phase (see Fig. 5 (D)). The Hololens2 application was compiled and deployed on the HMD as a standalone UWP developed in Unity 2019.4.14f1, XR SDK, and Microsoft Mixed Reality Toolkit 2.5.1 (MRTK). The standalone AR application communicates with cloud storage through an HTTP protocol and a stationary laptop through UDP/TCP sockets. The execution models can be selected and downloaded from the cloud during the fabrication phase through an integrated holographic UI (see Fig. 5 (E)). As soon as the geometry is downloaded from the HMD. XML elements are parsed into Unity Prefab Assets and instantiated in the augmented workspace as digital instructions. Notably, the illustrated data flow (Figs. 5) can work in both ways - from the laptop CAD model to HMD execution holograms and the other way around - reporting advancements and execution progress to a third-party device.

2.2. Tool-augmented retrofitting

The following section details the retrofitting procedures used to integrate the drill into the augmented fabrication environment. Although production drawings are available for modern electric tools, this may not always be constant. Tools may still be in production, and product design CAD models could be confidential and not publicly accessible. A reverse engineering logic was adopted to overcome these concerns and extend the resilience and validity of the retrofitting approach to a broad spectrum of tools. This procedure allows the use of outdated woodworking tools for efficient digital fabrication workflows. Thus, the tool's efficiency is boosted, and its life can be extended.

Scans of the drill were acquired using the same handheld 3D scanner. Scanning precision and correct point cloud postprocessing of an object are the primary factors for successful overlaying physical and virtual models. Another critical step consists of manufacturing and installing the camera mount on the tool. Three-dimensional printing of all the parts mitigates the risk of virtual–physical misalignments. A heavy fall or shock can change the physical position of a tracking camera. Thus, the resulting discrepancies between the physical and virtual drill models may eventually impose a retrofitting process from Phase B (see Fig. 6).

The tracking camera was equipped with a high-speed inertial measurement unit (IMU), two fish-eye image sensors, and a VPU processor ASIC. Using the acquired IMU data (magnetometer, gyroscope, and accelerometer), the tracking camera VIO can provide 6DoFs pose by comparing detected features from the left and right fish-eye sensors (see Fig. 7). Furthermore, the camera localization position is known by the factory and corresponds to the center of the left and right fish-eye sensors (see Fig. 8, A). The positioning and orientation of the tracking camera toward the right side of the drill are specific to right-handed users to ensure that the camera FOV is free of obstructions. Because the virtual drill model can be informed of the origin of the camera tracking plane (see Fig. 8, A), camera translation and rotation can be applied to the end of the drill bit (see Fig. 8, A'). With this

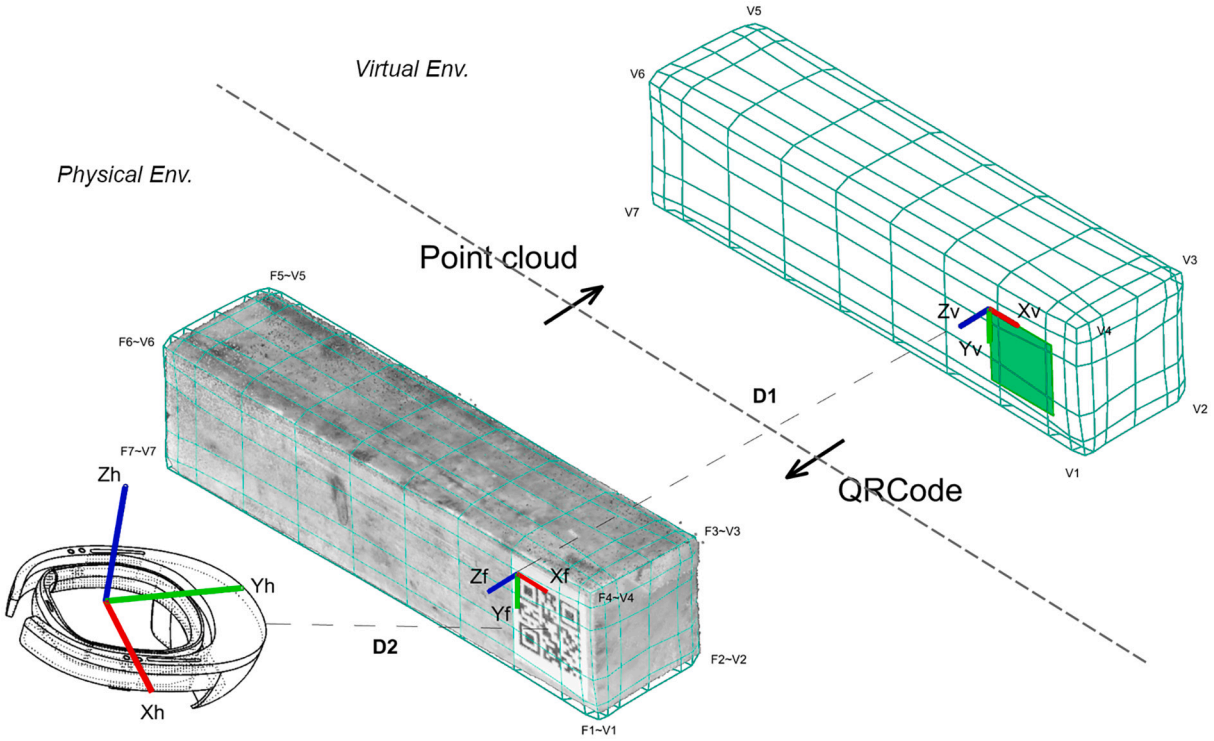

Fig. 4. Virtual and physical object alignment based on marker detection.

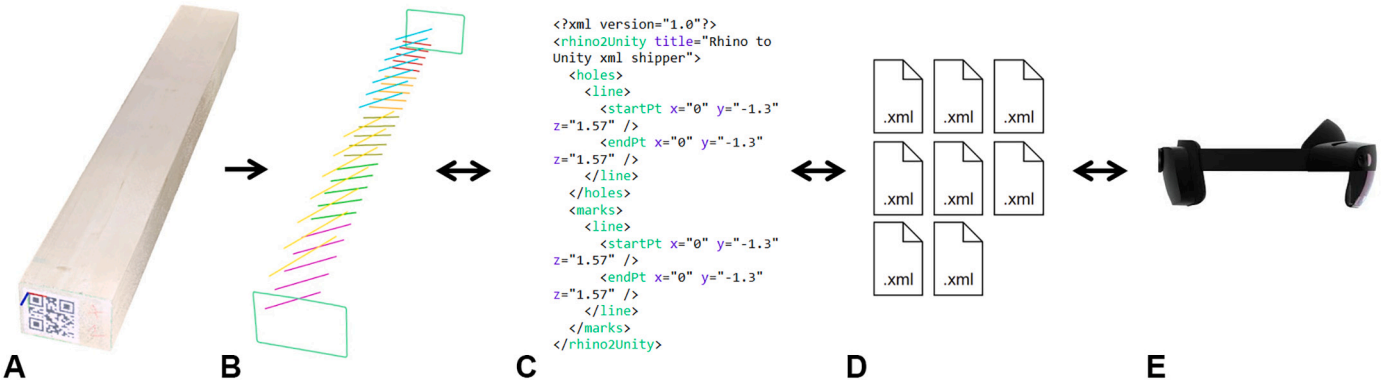

Fig. 5. Data flow from point cloud CAD to holographic execution models: (A) raw point cloud is processed, (B) CAD execution drawings for drilling and outlines are drawn from the point cloud model, (C) geometries are converted into an XML file for subsequent parsing, (D) XML files are uploaded on a cloud storage service, and (E) model is imported in the HMD and parsed into Unity Prefab Assets.

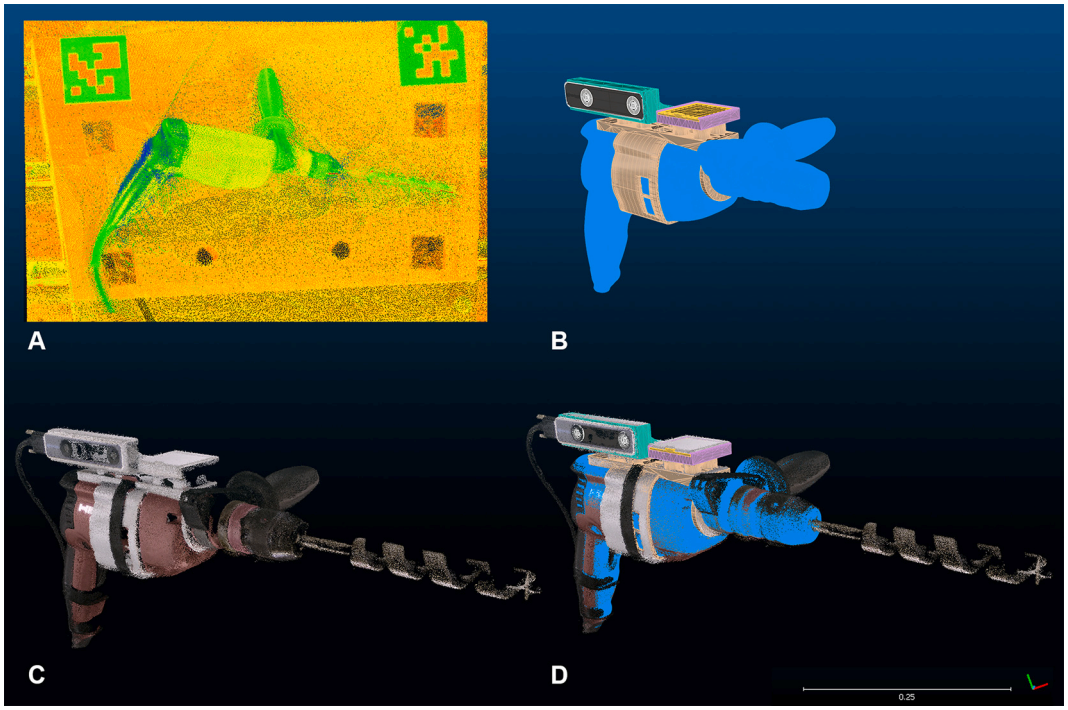

Fig. 6. Articulation of the drill retrofitting phases: (A) a raw point cloud is acquired from the drill using a handheld scanner, (B) the point cloud is processed into a mesh and used as a reference to design a camera mount, (C) all parts are 3D printed and installed on the drill, and (D) a final scan of the retrofitted drill is used to confirm a proper matching between the physical drill and its 3D model.

transformation, the virtual environment becomes aware of every drill movement at any time during the drilling process. The closed-loop drift factory value of the tracking camera, which informs us about the rate between the traveled distance and the amount of drift of the registered pose, was measured to be 1%. In practice, drifting events occur often and are caused by several factors: changing the environment or featureless surroundings, sudden movements, or very intense vibrations produced by the drill motor. A recalibration mechanism was implemented to quickly re-align physical and virtual drills in the case of severe tracking drift (see Fig. 9). By manually overlaying the physical tracking camera attached to the tool with its designated holographic template (see Fig. 10B), the physical and virtual drill models can be resynced at any time during fabrication. Although the recalibration of the drill position is highly influenced by the user capabilities of aligning the drill with its respective hologram, the IMU data feed can be correctly reset for use in live computations (see Fig. 8), and the holographic UI attached to the drill can again follow the drill displacement.

2.3. Augmented drilling

Manufacturing-specific holographic pads are integrated into the system to provide users with full accessibility to tool-camera sensors and user-parameter inputs (see Fig. 10), and drill recalibration (see Fig. 10B), execution model selection, and download from the cloud (see Fig. 10A).

When the pose stream of the tool is active, and the timber element and its virtual correspondent model are correctly overlaid, the assisted drilling operation can be initiated. The proposed AR framework can provide a feedback loop mechanism for drilling orientation and depth tracking to guide the user accurately during the correct execution of the hole. The tracking camera is connected to a stationary laptop that receives the drill-pose stream and transfers it to the HMD. The deviation

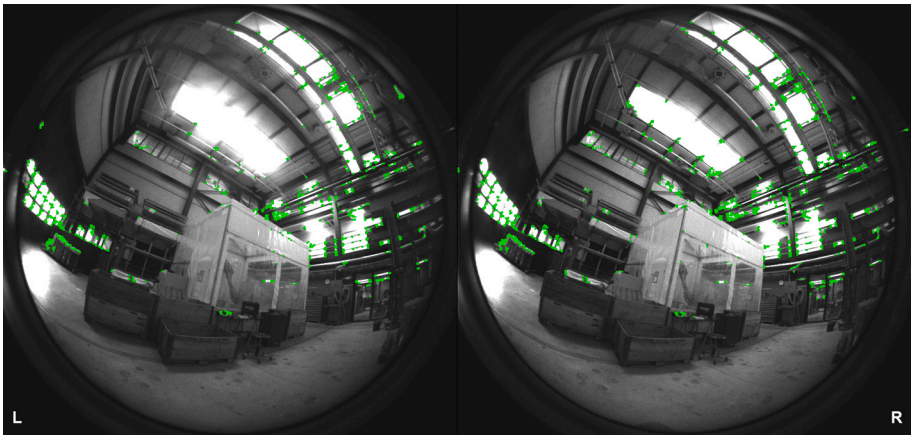

Fig. 7. Left and right fish-eye from the tracking camera. In green the "Harris Corner Features" as an example of features detection was used for visual inertial odometry systems. (For interpretation of the references to colour in this figure legend, the reader is referred to the web version of this article.)

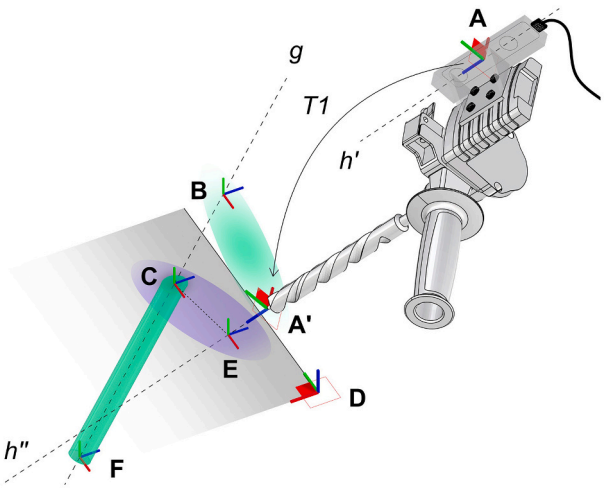

Fig. 8. Feedback looping logic of augmented drilling: (A) tracked camera position, (A') tracked tooltip position and plane, (B) intersection between tooltip plane and hole's axis, (C) hole's starting point, (D) top surface plane of the timber piece, (E) intersection between drill bit's axis and timber's top surface, (F) hole's ending point, (g) hole's axis, (h') tracking camera's orientation, (h") drill's axis, and (T1) the rigid transformation necessary to transpose the tracking camera's pose to obtain the respective one for the tooltip and drill.

between the drills (see Fig. 8, h" or h'), and hole axis (see Fig. 8, g) was computed in the HMD and parsed into a visual UI to guide and validate the user's adjustment. If not correct, the operator follows the graphical interface feedback (see Fig. 11C) until the angles BCE and ECA' are equal to zero (see Fig. 8). The same feedback logic is used for depth tracking. Specifically, its value corresponds to the live-computing intersection of the A' plane tooltip with the straight line f of the hole, as illustrated in Fig. 9. Finally, the starting point is the only value that is not integrated into the feedback loop. The overlaid holographic model is the only visual feedback to guide the user to accurately place the drill tip on the corresponding physical emplacement of the hole starting point (see Fig. 10B). In practice, the computed values for orientation and depth monitoring are parsed into a compact holographic HUD (see Fig. 10C). The augmented fabrication sequence is structured as follows: The drill is first calibrated with the augmented setup (see Fig. 9); next, the drill tip was pointed on the hologram corresponding to the hole starting point (see Fig. 11A), adjustments to the drill orientation concerning HUD angle feedback were applied (see Fig. 11B) when the drill orientation is correct (see Fig. 11C), the perforation can finally begin (see Fig. 11D). For depth-tracking guidance, a tracking bar is located on the right side of the holographic HUD (see Fig. 11E); when the hole is at its completion, the bar becomes fully green, and the user knows that he/she has reached the designated end for the current hole (see Fig. 11F).

In addition to collecting the tool-tracking camera stream, the stationary laptop also collects the updated 3D timber model 6DoFs pose from the HMD. By implementing the two pose streams into a shared CAD environment, such as Rhinoceros, a live-monitoring third-party interface application can be obtained. This companion live-overview interface can considerably oversee the progression of a particular manual task, contributing to efficient construction site management. Furthermore, this feature allows the 3D recording of data for human manufacturing operations. The drill tooltip path was recorded in a 3D coordinate system. Each passage is stored with the corresponding sequence time in a basic marked-up file for subsequent replay and inspection (see Fig. 12A). Data-driven recordings may provide new add-

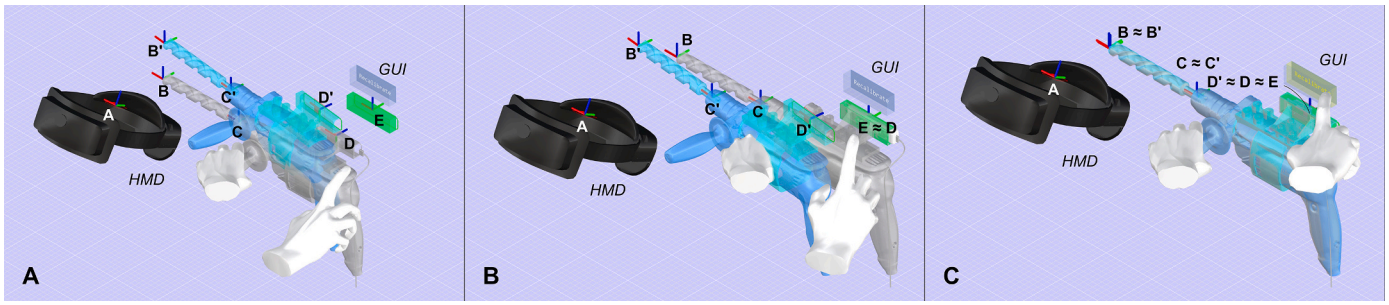

Fig. 9. Manual recalibration in tracking signal drifting: (A) SLAM drifting compromises the alignment of physical tool and virtual information, (B) user repositions the physical tool according to the holographic template, and (C) user confirms the recalibration, the tracking camera origin is synced with the correct physical position on the tool, and a new 6DoFs stream is adapted according to the new origin of the tool tracking system.

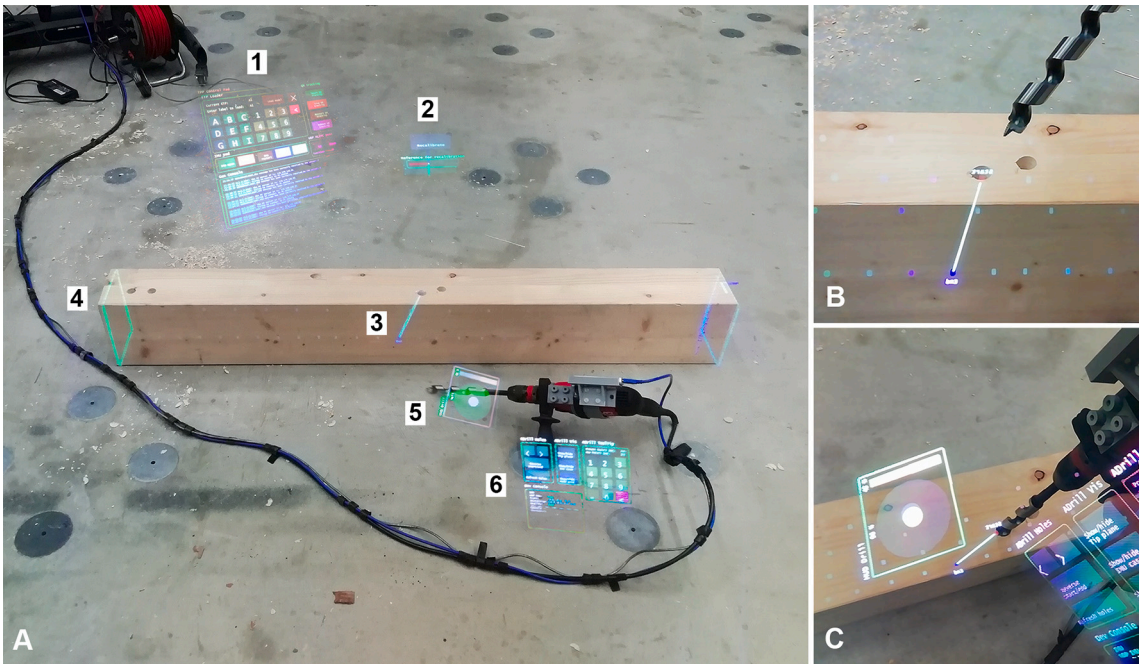

Fig. 10. View through the Hololens2 lenses of the holograms occupying the augmented carpentry workspace: (A.1) main control pad contains all GUIs for controlling the tracking camera, fiducial marker detection camera on the HMD, and downloading operations for the holographic shop drawings, (A.2) recalibration pad in case of lost tracking, (A.3 and B) holographic indication of the hole location, (A.4) minimal holographic outlines for virtual model overlaying visual check, (A.5 and C) holographic heads-up display (HUD) for drilling orientation and depth tracking, and (A.6) pad for drill specifics such as the drill bit length, selection of the designated hole to execute and IMU stream quality signal.

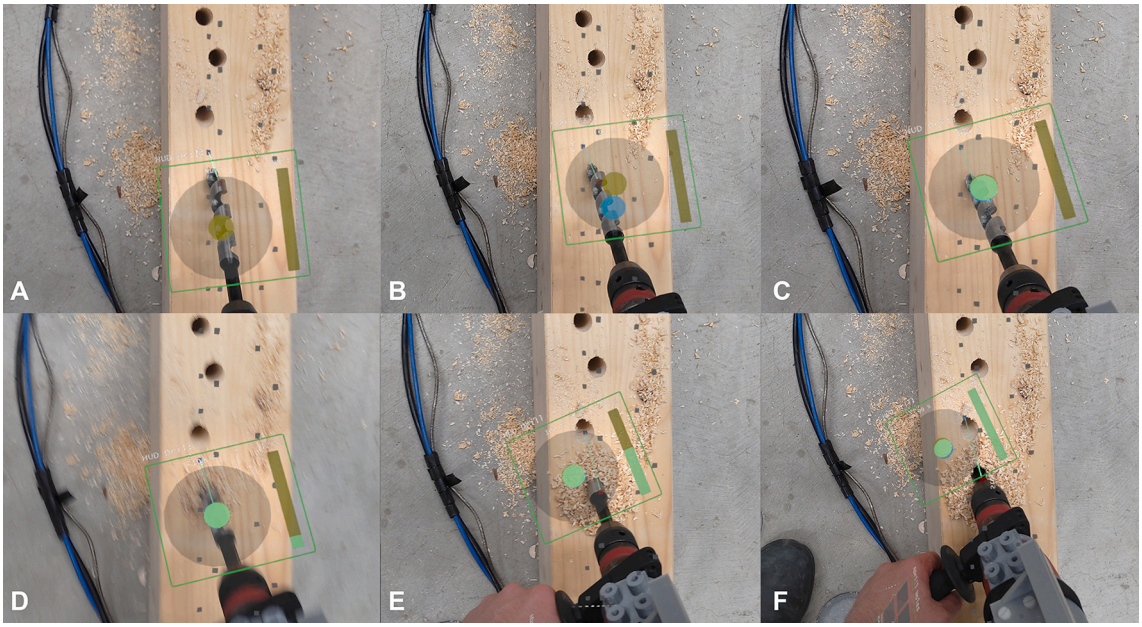

Fig. 11. Captured view of the tool HUD and UI through HMD lenses. Because of the integrated tracking camera SLAM, the drill GUI and HUD can seamlessly follow tool movement at any location in the workspace.

value to augmented human handcrafts in construction by certifying manufacturing quality through a Cartesian recording that can be archived and consulted later (see Fig. 12B). Furthermore, 3D tracked human operations on construction sites may become a resourceful digital asset that can save time and resources in settling quality-related execution issues among the actors involved in the construction process.

3. Evaluation and performance

3.1. Materials and methods

In the presented augmented drilling accuracy evaluation, the error between the as-drilled specimen and its corresponding 3D execution model is measured. In total, 224 holes were executed with angles ranging from 30 to 90° on sawn white spruce elements spanning from

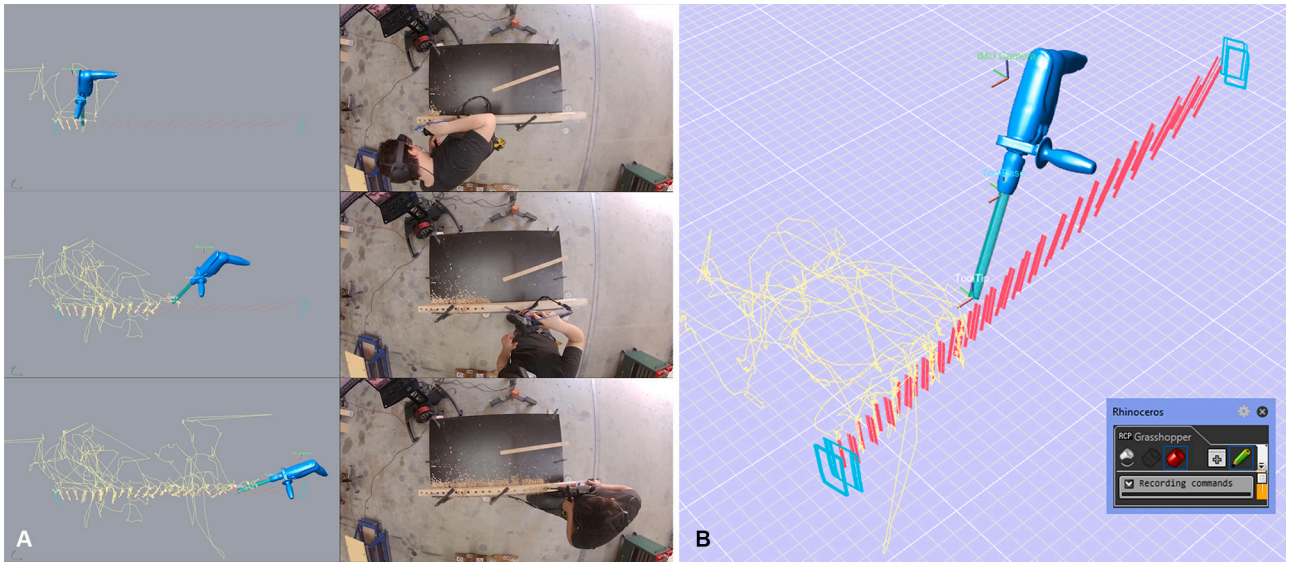

Fig. 12. (A) on the left, the augmented drill tool path is visualized live on a third-party screen and stored as a text file. On the right, a video recording of the physical execution. (B) Sequencing of the 3D recorded fabrication session within Grasshopper: both drill paths (yellow) and each timber piece movement (red and blue) were recorded in 3D coordinates. These two parameters can be inspected every 30 ms during the entire fabrication session.

1.2 to 1.8 m. The drilling depths were between 80 and 170 mm, with a similar distribution between each drilling angle. A specific drill for wood was used with one tracer and threaded tip, a 20-mm diameter with a continuous cylindrical shaft, and a total length of 200 mm. The same drilling machine, HILTI® SR-16, weighing approximately weighing 2.4 kg was used for all the specimens. Since this study represents only a pre-evaluation of this technology, only one user drilled all the holes. In the future, with an improved version of the augmented fabrication system,

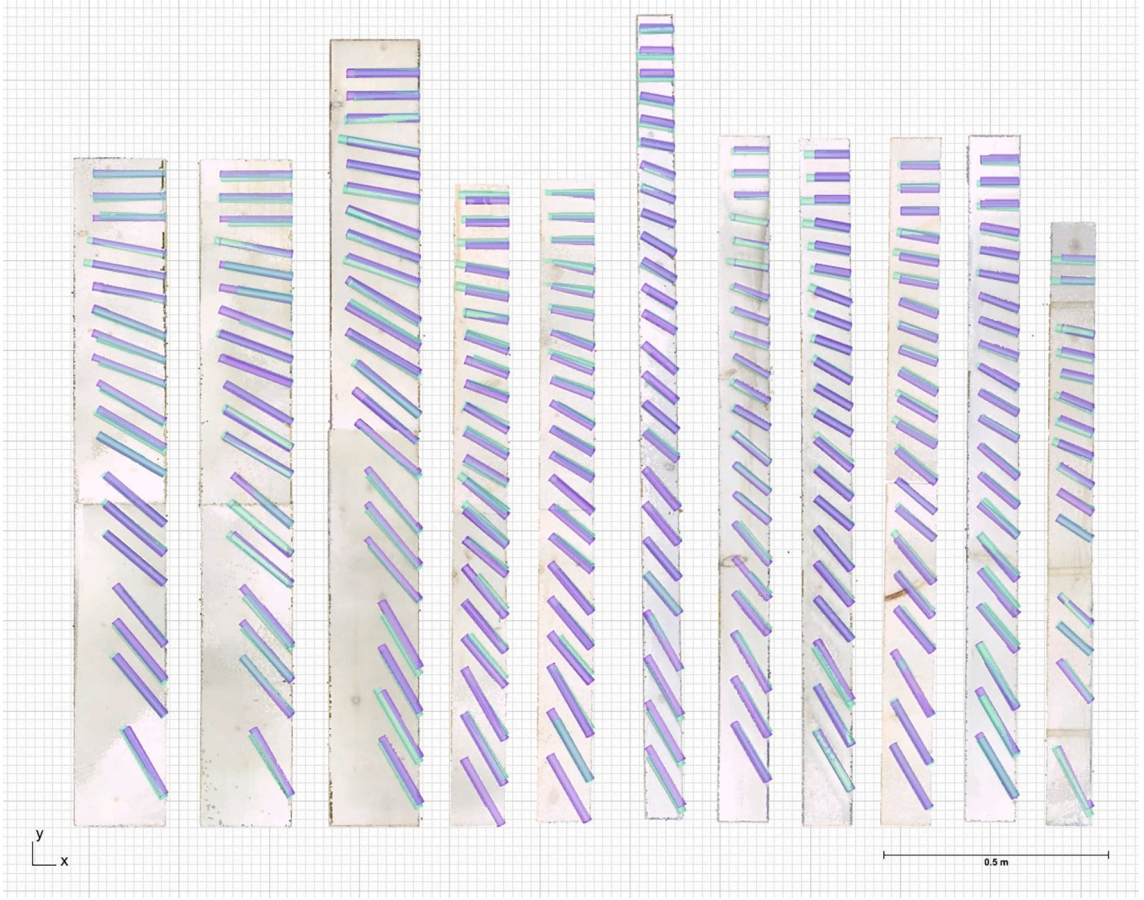

Fig. 13. Point cloud postprocessing results of split artifacts from one timber batch in a CAD environment: in green, the as-drilled holes, whereas in violet, the holes referring to the execution model. (For interpretation of the references to colour in this figure legend, the reader is referred to the web version of this article.)

the influence of various user types should be considered in an exhaustive experimental study.

To evaluate the holes made by the user, the specimens were sawn in half to reveal the cross-section of the holes. Next, 3D scanning was performed with a handheld scanner to obtain digital copies of each hole made in point cloud formats. Hole detection in the point cloud was fundamental to obtaining correct modeling of the physical specimen. A cylindrical quadrangular mesh with an appropriate radius for the corresponding hole was first sampled as a point cloud. Next, the user manually suggested a rough approximation of the hole position and orientation. The hole positioning was finally refined by an iterative closest point (ICP) registration method to obtain an accurate prediction of real-world perforation (see Fig. 13). When the positions and orientations of the holes were identified, the as-drilled and execution models were overlaid for comparison. Similar to the previous phase, a random sample consensus method was combined with ICP refinement to register the two models accurately. At this point, virtual–physical deviations were manually measured for each drilling with respect to four parameters: 1) the distance between the two entry points, named the starting point error (see Fig. 14, A and B); 2) the angle difference between the axis of the two holes, named the orientation error (see Fig. 14, a and b); 3) the difference between the two drilling lengths, called the depth error (see Fig. 14, AA' and BB'), and 4) the distance between the two termination points, called the ending point error (see Fig. 14, A' and B′). Point clouds from 3D scans and reconstructed 3D data are available in the open-access data repository [23].

3.2. Results and discussions

In this section, the errors of each parameter listed below are represented by their mean values and standard deviations, as listed in Table 1. In addition, Fig. 15 displays the variation in the absolute errors in the form of boxplots for each parameter. All experimental data and statistical analyses are available in the open-access data repository [23].

Regarding the starting point and orientation error, which are the entry parameters before starting drilling, the error increases when the angle is small, with maximum errors for angles of 30° and 40°. The variation of the error is critical for drillings made at 30°, whereas for the other angles, the variation is rather equal, with minimum values for the angles of 60 and 70° (see Fig. 15, A and B). The small angles, therefore, influence in part the accuracy of the starting point but also the accuracy of the orientation. For the starting point, occasional holographic drifting and imprecision in the timber virtual model overlaying are accountable for the high values of entry point deviances. Point cloud pre-processing QR plane detection can already add sub-millimeter imprecision to the physical and virtual object overlapping mechanism. Furthermore, in the subsequent QR plane detection of the same fiducial marker, additional tolerances can be added to the existing ones, which results in misleading feedback to identify the correct entry point and angle. Notably, even the slightest perceived misalignment of the physical object and virtual 3D model can result in imprecision for other drilling feedback. Although multiple fiducial markers could improve alignment accuracy, preparation and detection may result in impractical and laborious work. Therefore, future developments should focus on intuitive and markerless solutions for virtual physical object calibration. For orientation feedback at small angles close to 30°, holes should be first started vertically and then, while drilling, quickly adjusted to the correct orientation. Such abrupt but necessary movements can result in consistent inaccuracies. Nonetheless, the gyroscope sensor integrated into the tool camera's high-speed IMU unit revealed that it can provide reliable information to

Table 1
Error in position for various experimental parameters.

Drilling angle	Number of specimens	Starting point error	Orientation error	Depth error	Ending point error
(°)	(–)	(mm)	(°)	(mm)	(mm)
30	27	8.37 ± 4.78	1.90 ± 1.21	10.74 ± 7.40	13.30 ± 6.93
40	32	8.00 ± 3.64	1.83 ± 0.92	12.44 ± 11.47	13.53 ± 8.65
50	33	5.94 ± 3.77	1.64 ± 1.31	6.79 ± 5.62	10.15 ± 5.33
60	34	6.06 ± 3.12	1.29 ± 1.14	4.76 ± 3.37	8.21 ± 3.73
70	33	5.30 ± 2.39	1.40 ± 0.76	8.21 ± 8.70	10.58 ± 8.43
80	33	5.03 ± 2.91	1.28 ± 0.97	11.97 ± 8.55	14.21 ± 8.11
90	32	6.28 ± 2.95	1.30 ± 0.64	9.72 ± 8.03	12.94 ± 6.96
Total	224	6.37 ± 3.55	1.51 ± 1.03	9.16 ± 8.26	11.78 ± 7.27

* The errors are represented as mean ± standard deviation.

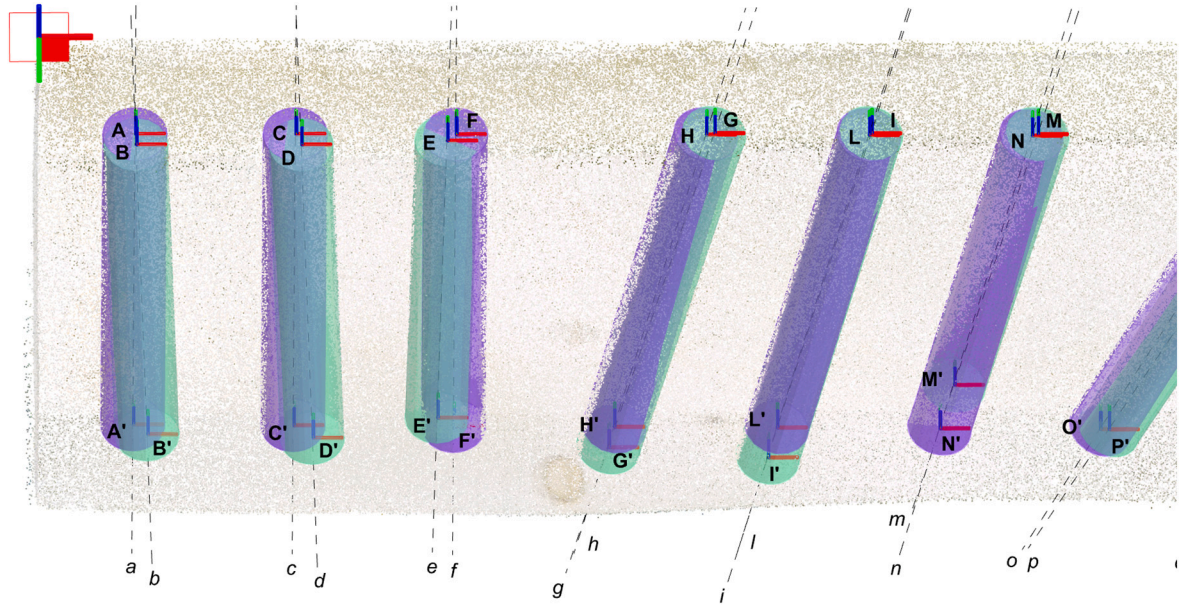

Fig. 14. Portion of the post-processed point cloud of the timber element longitudinal section.

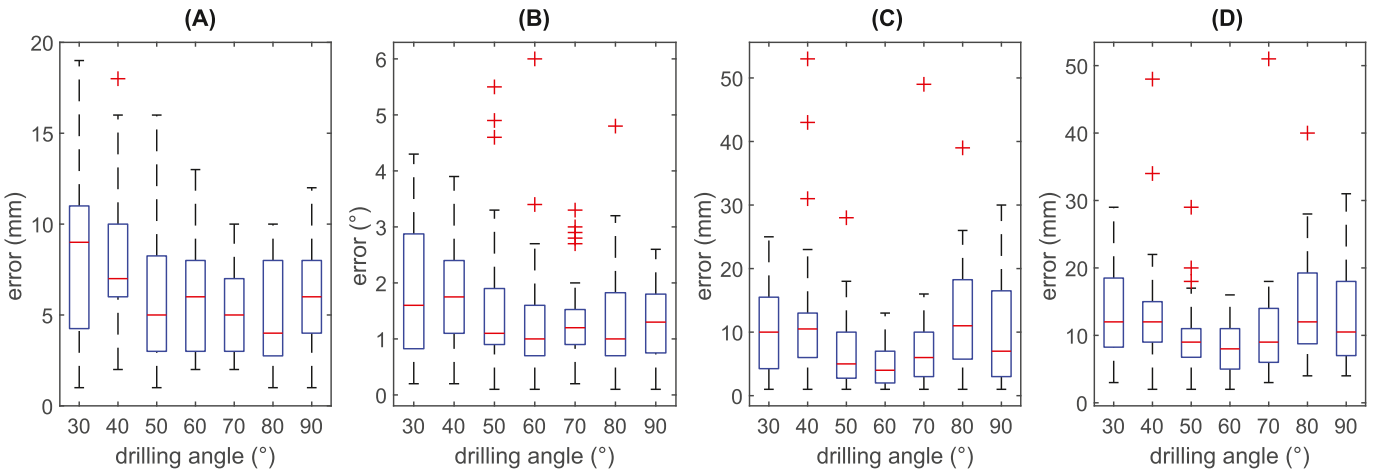

Fig. 15. Boxplots of the error for each parameter: (A) starting point error, (B) orientation error, (C) depth error, and (D) ending point error. On each box, the central mark indicates the median, and the bottom and top edges of the box indicate the 25th and 75th percentiles, respectively. The whiskers that extend to the most extreme data points are not considered outliers, and the outliers are plotted individually using the + symbol.

the user with robust feedback of the tool orientation. The mean error for all the drillings was 6.37 ± 3.5 mm for the starting point and 1.51 ± 1.0° for the orientation.

Regarding the depth error, which is partially influenced by the progressive accumulation of tolerances belonging to the orientation parameter and the entry point, the error has minimum values for angles between 50 and 70°, which also exhibits a minimum variation, as displayed in Fig. 15C. The preferential position of the tool holder at such angles is a possible explanation for these results. For the other angles, the error was higher in the same range with a larger variation. The realignment method can be considered accountable for adding tolerances to the depth feedback accuracy, depending on the user performance in overlaying the physical tool with the holographic template for recalibration (see Fig. 9). For the most part, drilling depth imprecision can occasionally be caused by erroneous guidance based on the position localization of the V-SLAM feed. Despite excellent resistance to drilling vibrations, drifting events in tracking often occur, which hinders the system from providing correct depth information for user guidance. In this specific tool tracking application, the inside-out positional localization requires higher precision than, for example, larger autonomous robots for which many SLAM systems are currently being developed. Nevertheless, implementing light detection and ranging SLAM can improve the precision and accuracy of the self-tracking drill position, especially when coupled with other companion sensors. For now, the mean error for all the drillings is 9.16 ± 8.26 mm for the depth length. The standard deviation is high for all parameters, but especially for the depth error with a standard deviation almost equal to the mean error value. Therefore, future improvements in this parameter should facilitate a considerable overall upgrade of this augmented framework.

Finally, the ending point error can be attributed to all errors of the previous parameters. Therefore, the overall accuracy could be expressed as the mean error on all the drillings for this parameter and is 11.78 ± 7.27 mm. Furthermore, the coefficient of variation is approximately 60%, which indicates inadequate reproducibility and consistency. This result can be attributed to human and technological factors and will be evaluated in a future experimental campaign when all enhancements have been added to this fabrication methodology.

4. Conclusions

This study investigated the potential of AR technologies to enhance human performance in volume subtractive manual tasks, such as drilling. The retrofitting procedures to augment and integrate an ordinary electric drill into a design-to-fabrication augmented workflow was demonstrated with an HMD as the main UI. The upcycling of such common tools contributes to the sustainability of the presented manufacturing system. The system showcases the versatility of an inside-out tracking system for manual tool path localization, monitoring, and recording. A craft-specific interface was successfully designed to ease the user capacity to follow explicitly computed feedback from the augmented framework and complement them with implicit human corrections. With this first proof of concept, the preliminary results revealed the capacity of a general user to successfully follow specific drilling trajectories without the requirement for jigs or physical guides. The experimental evaluation using 3D scanning techniques resulted in an estimated precision of approximately 10 mm with high variance.

Therefore, several optimization methods can be investigated based on these initial results. First, to improve the drilling starting point, the system requires a markerless or intuitive and accurate timber element calibration mechanism that does not require preliminary scanning of the piece. Second, depth tracking also has margins for improvement because it is too heavily dependent on the imprecise SLAM positional feed of the tracking camera. Therefore, in the future, a dedicated visual monitoring system uniquely in charge of observing the tooltip area to deduce depth data, among other information, should be developed. Third, multiple methods can be investigated for guidance systems. Although the use of the HMD represents a light cognitive load for the operator, it also presents some shortcomings in the accuracy and stability of the holograms. New interfaces could also leverage senses other than the view to provide alternative user-hands-free guidance [24]. Fourth, each drilling parameter (e.g., orientation, depth, and entry point) is influenced by multiple data streams simultaneously, rendering the system brittle and prone to error accumulation. Future studies should consider thoroughly compartmentalizing the data streams and computed feedback. A comparative study among populations of users with various skill levels can provide a comprehensive view of the capacity of AR applications to bridge knowledge gaps in woodworking tasks.

Finally, the authors emphasize that augmented subtractive fabrication with intelligent tools should be complementary to factory-based robotic prefabrication. Site-based woodworking tasks (e.g., renovation of buildings or in situ adjustments) could benefit from agile and digitally enhanced fabrication systems that can be used in unstructured environments. Furthermore, independent participants in collective projects involving timber construction can gain the expertise necessary to integrate the design and the construction phase. With the implementation of the identified improvements, such a hybrid fabrication format can also be integrated into complementary digital manufacturing models for

timber to enhance automated workflow flexibility and simultaneously provide an asset digitization opportunity to small companies with low-level entry technology by leveraging the already present human workforce and pre-existing manual tools.

CRediT authorship contribution statement

Andrea Settimi: Conceptualization, Methodology, Software, Validation, Formal analysis, Investigation, Data curation, Writing – original draft, Visualization. **Julien Gamerro:** Conceptualization, Methodology, Validation, Formal analysis, Investigation, Resources, Data curation, Writing – original draft, Visualization, Supervision, Project administration, Funding acquisition. **Yves Weinand:** Resources, Supervision, Funding acquisition.

Declaration of Competing Interest

None.

Acknowledgments

The authors would like to acknowledge the financial support of the École Polytechnique Fédérale de Lausanne (EPFL) and, in particular, the ENAC Faculty with the Cluster Grant, which partially contributed to obtaining the necessary equipment. This study did not receive any external funding. The authors also thank the Structural Engineering Group of the EPFL for their support and assistance.

Appendix A. Supplementary data

Supplementary data to this article can be found online at https://doi.org/10.1016/j.autcon.2022.104272.

References

[1] Y. Song, R. Koeck, S. Luo, Review and analysis of augmented reality (AR) literature for digital fabrication in architecture, Autom. Constr. 128 (2021), 103762, https://doi.org/10.1016/j.autcon.2021.103762.
[2] M. Chu, J. Matthews, P.E.D. Love, Integrating mobile building information modelling and augmented reality systems: an experimental study, Autom. Constr. 85 (2018) 305–316, https://doi.org/10.1016/j.autcon.2017.10.032.
[3] G. Jahn, C. Newnham, N. Berg, M. Iraheta, J. Wells, Holographic Construction, Springer International Publishing, 2020, pp. 314–324, https://doi.org/10.1007/978-3-030-29829-6_25. Ch. 10.
[4] D. Mitterberger, K. Dörfler, T. Sandy, F. Salveridou, M. Hutter, F. Gramazio, M. Kohler, Augmented bricklaying: human–machine interaction for in situ assembly of complex brickwork using object-aware augmented reality, Construct. Robot. (2020), https://doi.org/10.1007/s41693-020-00035-8.
[5] T. Kuzhagaliyev, N.T. Clancy, M. Janatka, K. Tchaka, F. Vasconcelos, M. J. Clarkson, K.S. Gurusamy, D.J. Hawkes, B.R. Davidson, D. Stoyanov, Medical Imaging: Image-Guided Procedures - Augmented Reality Needle Ablation Guidance Tool for Irreversible Electroporation in the Pancreas 10576, March 2018, https://doi.org/10.1117/12.2293671.
[6] C. Kunz, P. Maurer, F. Kees, P. Henrich, C. Marzi, M. Hlaváč, M. Schneider, F. Mathis-Ullrich, Infrared marker tracking with the HoloLens for neurosurgical interventions, Curr. Direct. Biomed. Eng. 6 (1) (2020) 20200027, https://doi.org/10.1515/cdbme-2020-0027.
[7] G. Brugnaro, S. Hanna, Adaptive robotic carving, in: J. Willmann, P. Block, M. Hutter, K. Byrne, T. Schork (Eds.), Robotic Fabrication in Architecture, Art and Design 2018, Springer International Publishing, Cham, 2019, pp. 336–348, https://doi.org/10.1007/978-3-319-92294-2_26.
[8] P. Kriechling, S. Roner, F. Liebmann, F. Casari, P. Fürnstahl, K. Wieser, Augmented reality for base plate component placement in reverse total shoulder arthroplasty: a feasibility study, Arch. Orthop. Trauma Surg. (2020), https://doi.org/10.1007/s00402-020-03542-z.
[9] P.-C. Wu, R. Wang, K. Kin, C. Twigg, S. Han, M.-H. Yang, S.-Y. Chien, DodecaPen: accurate 6DoF tracking of a passive stylus, in: Proceedings of the 30th Annual ACM Symposium on User Interface Software and Technology, UIST '17, Association for Computing Machinery, New York, NY, USA, 2017, pp. 365–374, https://doi.org/10.1145/3126594.3126664.
[10] H. Liu, E. Auvinet, J. Giles, F. Baena, Augmented reality based navigation for computer assisted hip resurfacing: a proof of concept study, Ann. Biomed. Eng. 46 (2018), https://doi.org/10.1007/s10439-018-2055-1.
[11] A. Zoran, R. Shilkrot, S. Nanyakkara, J. Paradiso, The hybrid artisans: a case study in smart tools, ACM Trans. Comput. Hum. Interact. 21 (3) (2014) Jun, https://doi.org/10.1145/2617570.
[12] T. Müller, Designing with Haptic Feedback, Master's thesis, Umeå University, Umeå Institute of Design, 2020, http://www.uid.umu.se/en/uid20/project-gallery/apd/thomas-mueller/. last accessed on 2021-10-28.
[13] Intuity Media Lab GmbH, Active Haptics in Smart Tools. https://www.intuity.de/en/projekte/intuity-haptik-demonstrator/, 2022 last accessed on 2021-10-24.
[14] Shaper, Shaper Origin Tool Website. https://www.shapertools.com/, 2022 last accessed on 2021-10-24.
[15] S. Kawabata, J.H. Lee, S. Okamoto, Obstacle avoidance navigation using horizontal movement for a drone flying in indoor environment, in: 2019 International Conference on Control, Artificial Intelligence, Robotics Optimization (ICCAIRO), 2019, pp. 1–6, https://doi.org/10.1109/ICCAIRO47923.2019.00009.
[16] E. Tsykunov, V. Ilin, S. Perminov, A. Fedoseev, E. Zainulina, Coupling of Localization and Depth Data For Mapping Using Intel Realsense T265 and d435i Cameras, CoRR abs/2004.00269, 2020. arXiv:2004.00269.
[17] T.H. Henri Rebecq, D. Scaramuzza, Real-time visual-inertial odometry for event cameras using Keyframe-based nonlinear optimization, in: G.B. Tae-Kyun Kim, Stefanos Zafeiriou, K. Mikolajczyk (Eds.), Proceedings of the British Machine Vision Conference (BMVC), BMVA Press, 2017, pp. 16.1–16.12, https://doi.org/10.5244/C.31.16.
[18] AHA & ESA Use Holographic Guides with a Chainsaw for a Furniture Project. https://hidakuma.com/en/blog/20210331_torinosu/, 2020 last accessed on 2021-10-26.
[19] Tracking Camera t265 / t261 Datasheet, Intel® RealSense™ Developer Documentation. https://dev.intelrealsense.com/docs/tracking-camera-t265-datasheet, 2022 last accessed on 2021-07-19.
[20] P. Vestartas, A. Settimi, Cockroach: A Plug-in for Point Cloud Post-processing and Meshing in Rhino Environment. https://github.com/ibois-epfl/Cockroach, 2020 last accessed on 2021-10-02.
[21] R. Hughes, T. Osterlund, N.M. Larsen, Integrated design-for-manufacturing and AR-aided-assembly workflows for lightweight reciprocal frame timber structures, construction, Robotics (2021), https://doi.org/10.1007/s41693-020-00048-3 (2021-06-26).
[22] C. Parry, S. Guy, Recycling construction waste material with the use of AR, in: P. F. Yuan, J. Yao, C. Yan, X. Wang, N. Leach (Eds.), Proceedings of the 2020 DigitalFUTURES, Springer Singapore, Singapore, 2021, pp. 57–67, https://doi.org/10.1007/978-981-33-4400-6_6.
[23] A. Settimi, J. Gamerro, Y. Weinand, Supplementary material for "AR-assisted timber drilling with smart retrofitted tools", V3 Zenodo (Jul. 2021) https://doi.org/10.5281/zenodo.5142178.
[24] M. Larsson, H. Yoshida, T. Igarashi, Human-in-the-loop fabrication of 3D surfaces with natural tree branches, in: Proceedings of the ACM Symposium on Computational Fabrication, SCF '19, Association for Computing Machinery, New York, NY, USA, 2019, https://doi.org/10.1145/3328939.3329000.